Metastable Triply Charged Diatomic Molecules Produced with Femtosecond Pulses

Hirofumi Sakai,[1,2] H. Stapelfeldt,[1,*] E. Constant,[1,†] M. Yu. Ivanov,[1] Daniel R. Matusek,[3]
James S. Wright,[3] and P. B. Corkum[1]

[1]*Steacie Institute for Molecular Sciences, National Research Council of Canada, Ottawa, Ontario, Canada K1A 0R6*
[2]*Optoelectronics Division, Electrotechnical Laboratory, 1-1-4, Umezono, Tsukuba, Ibaraki 305, Japan*
[3]*Ottawa-Carleton Chemistry Institute, Carleton University, Ottawa, Ontario, Canada K1S 5B6*
(Received 28 February 1997)

We show that ultrashort pulse strong field multiphoton ionization efficiently produces *metastable* highly charged molecules such as metastable diatomic trications I_2^{3+}, Br_2^{3+}, and Cl_2^{3+}. The efficiency of stable trication production decreases rapidly with increasing pulse duration. Weak pre- or post-pulse irradiation also prevents efficient production or survival of trications. We propose strong-field femtosecond Raman spectroscopy to determine trication vibrational frequencies.   [S0031-9007(98)07113-0]

PACS numbers: 33.80.Rv, 31.15.−p, 36.10.−k

In the tunneling limit [1] of multiphoton atomic ionization, the laser field oscillates so slowly that electrons adiabatically adjust to the field. Only the most weakly bound electron can tunnel through the oscillating barrier created by the laser field and the binding potential. Together with the high efficiency of multiphoton ionization, this has led to the application of atomic multiphoton ionization to producing highly controlled plasmas and new gain media for x-ray lasers [2].

In molecules, because of the large disparity between the electron and nuclear masses, adiabaticity for the electrons can be combined with almost frozen nuclear motion [3] provided very short laser pulses are used. If tunnel ionization remains efficient and gentle, strong fields provide an alternative ionization source in mass spectrometry [4] where improving the sensitivity requires minimum fragmentation of the molecule and maximum ionization efficiency.

We demonstrate the gentleness of the strong field ionization process by producing triply charged diatomic halogen molecules. In these molecules removal of three electrons increases the bond order leading to weakly metastable ground states [5–7], but otherwise repulsive potential curves. We demonstrate the necessity of very short pulses by showing that these molecular ions are not produced when the pulse duration is increased. They are also shown to be very sensitive to relatively weak pump or probe pulses. The lifetime of these metastable trications can exceed 10^4 years.

The laser system used in the experiment produced near diffraction limited and transform limited 80 fs, 200 μJ, 625 nm pulses [8]. These pulses were divided into two parts in a Michelson interferometer, producing a main pulse and pre- or post-pulses (if needed for the experiment). The intensity of the (weaker) pre- or post-pulse was controlled with a variable aperture.

The pulses were focused inside a vacuum chamber to a focal spot of approximately 10 μm in diameter. The target chamber was fitted with a gas jet (nozzle diameter 250 μm) [8] with the jet axis perpendicular to the axis of the laser beam, intersecting it 8 cm from the nozzle. The main role of the jet was to ensure that the molecular ions had very little initial velocity (the estimated transverse energy is less than 10^{-6} eV) in the flight direction leading to easily identified time-of-flight (TOF) peaks. This allows us to differentiate fragmented from nonfragmented ions by the sharpness of the TOF peaks. Typical partial pressures used to back the jet were 0.3 Torr I_2, 760 Torr He; 20 Torr Br_2, 230 Torr He, 50 Torr Cl_2, 150 Torr He.

The time-of-flight chamber with TOF axis perpendicular to the jet axis and to the direction of propagation of the laser beam was described previously [8,9]. It consisted of an accelerating region with a 250–533 V/cm electric field and a field-free drift region. In our TOF design we favored detection of intact molecular ions over the more numerous dissociating molecular ions. Fragments from the latter acquire a large velocity during dissociation and if only a small component of this velocity is perpendicular to the flight axis they cannot reach the microchannel plate through the 0.5 mm aperture in the TOF electrode.

Figure 1 shows the TOF mass spectrum for all three metastable trications. The typical peak laser intensity used was $(1-5) \times 10^{14}$ W/cm². Figure 1(a) shows the peak at the position corresponding to I_2^{3+}. The TOF peak corresponds to a mass-to-charge ratio of 84.59; the anticipated value is 84.60. Figures 1(b) and 1(c) show the results for Br_2^{3+} and Cl_2^{3+}. All peak widths are imposed by the time resolution limit of our system. The peaks must arise from molecular ions since any photodissociation event necessarily broadens the peak beyond our few μeV resolution. All peaks are observed at precisely the arrival times expected for the trication and have the isotope ratios that agree with the anticipated ratios within the experimental accuracy of about 20%. The results were independent of whether the light is linearly or circularly polarized.

Although our experiment was not designed to precisely measure the efficiency of trication production, we can
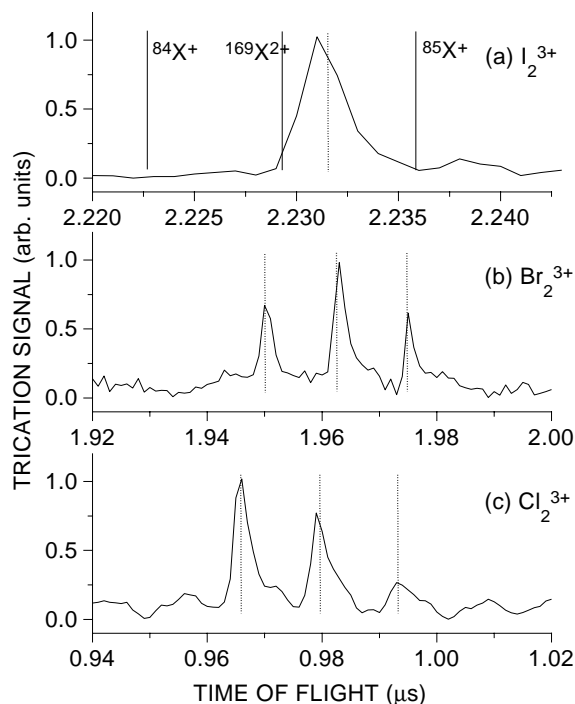
FIG. 1. Selected portions of the time-of-flight spectra showing peaks of I_2^{3+} (a), Br_2^{3+} (b), and Cl_2^{3+} (c). Dotted lines show anticipated positions of trications calibrated with well-known species. Positions of the singly charged mass 84 and 85 peaks and the position of the doubly charged mass 169 are included in (a) for reference.

estimate it from the area under the peaks corresponding to metastable and dissociating trications in the TOF spectrum, i.e., areas under I_2^{3+} and the $I^+ + I^{2+}$ peaks for iodine. This underestimates the metastable channel since $I^+ + I^{2+}$ can be produced from a larger ionization volume due to enhanced ionization [10,11]. Correcting for the collection efficiency, we observe the ratio of bound to dissociating channels of I_2^{3+} between 1:450 to 1:1200. Large fluctuations in the measured ratio are due to fluctuations in a relatively small I_2^{3+} signal, which is typical for highly nonlinear processes.

Figure 2 shows the calculated metastable ground state and some of the low-lying excited states of Cl_2^{3+}. To perform these calculations, we used the nonrelativistic multireference configuration interaction method of Buenker and co-workers [12]. The Gaussian basis set using the contraction $(14s10p2d/11s7p2d)$ was taken from [13]. The electron configuration of Cl_2^{3+} near its ground-state potential minimum is expected to be $\dots (\pi_u)^4 (\pi_g)^1$, corresponding to the removal of three electrons from the $(\pi_g)^4$ configuration in ground state Cl_2. However, at larger distances there is strong configuration mixing with more open-shell configurations of the type $\dots (\pi_u)^2 (\pi_g)^2 (\sigma_u)^1$. This configuration was used to generate the orbitals for the configuration interaction in all electronic states at the self-consistent field stage of the calculation.
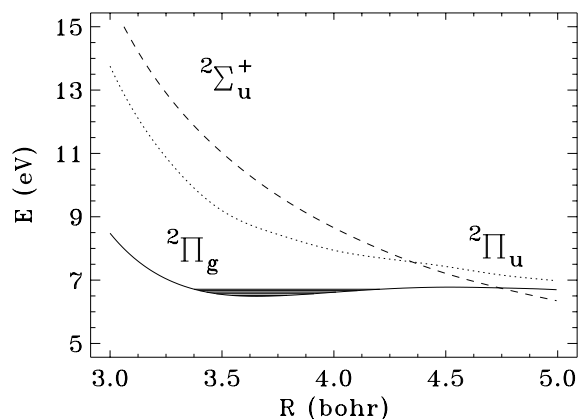

FIG. 2. Calculated ground and low-lying potential curves for Cl_2^{3+} with metastable vibrational states.

We considered the doublet states $^2\Pi_{g,u}$, $^2\Sigma_u^+$, $^2\Delta_u$, and $^2\Phi_{g,u}$ which include the states corresponding to the two lowest dissociative channels of doublet spin. The calculations typically included about 60 reference configurations and up to 7 roots, generating ca. 3.2×10^6 symmetry-adapted functions, from which $30\,000–55\,000$ were selected. This led to total reference configuration weights (i.e., $\sum c_i^2$) of $0.89–0.94$ for the ground state.

The potential well has a calculated depth of 0.288 eV and supports five ($v = 0–4$) metastable vibrational states (see Fig. 2) with the $0 \rightarrow 1$ transition at approximately 0.054 eV. The tunneling lifetimes are $\tau(v = 0) \approx 6.6 \times 10^4$ yr, $\tau(v = 1) \approx 0.2$ yr, $\tau(v = 2) \approx 71$ s, $\tau(v = 3) \approx 2.3 \times 10^{-3}$ s, $\tau(v = 4) \approx 1.6 \times 10^{-7}$ s. Note the very long tunneling lifetime of the ground vibrational state.

The equilibrium position of Cl_2^{3+} is $R_e^{(3+)} \approx 1.94$ Å, very close to that of the ground-state molecule, $R_e^{(0)} = 1.99$ Å. Similarly, for I_2^{3+} $R_e^{(3+)} \approx 2.84$ Å and $R_e^{(0)} = 2.66$ Å. Vertical transition from the $v = 0$ state of Cl_2 to the ground electronic surface of Cl_2^{3+} yields the following populations of the vibrational states: $P(v = 0) \approx 77.4\%$, $P(v = 1) \approx 22.1\%$, $P(v \geq 2) \approx 0.5\%$.

The efficiency of metastable trication formation decreases rapidly as the molecuar mass decreases. Ideally, ionization should proceed quickly compared to typical vibrational time scales of the molecule. For the three trications that we observed this condition was reasonably well met by our 80 fs pulse (ground state vibrational periods are 157 fs for I_2, 103 fs for Br_2, and 60 fs for Cl_2). On the contrary, we did not observe metastable trications for molecules with vibrational period much shorter than the pulse duration. For instance, metastable states have been predicted for N_2^{3+} [14]. However, the vibrational period of N_2 is only about 14 fs, so the internuclear separation can change significantly during the time required to remove the three electrons. We did not observe N_2^{3+} experimentally.

We have investigated the importance of the pulse duration in two ways. First, we studied production of I_2^{3+}

as a function of the pulse duration. We lengthened the pulse by placing dispersive media such as SF6 or SFL6 glass in the beam path, keeping the laser intensity constant at 3.6×10^{14} W/cm². The results are shown in Fig. 3. The formation of I_2^{3+} drops rapidly as the pulse duration is increased and at a duration of 330 fs we observe virtually no I_2^{3+}. Similar results were found for Br₂.

Second, we used a main pulse to produce I_2^{3+} and a pre- or post-pulse with intensity of about 1/3 of the main pulse to interact with either I₂ or I_2^{3+}. With only a pre- or post-pulse, the I_2^{3+} signal was very small. Figure 3 shows the I_2^{3+} signal plotted as a function of the delay between main and pre- or post-pulses. The signal at zero delay corresponds to that obtained with only the main pulse. We see that a weak pre- or post-pulse prevents efficient production or survival of I_2^{3+}.

Our observations when a pre-pulse was used are consistent with the following interpretation: A pre-pulse excites iodine molecules from the ground state, leading to a formation of a dissociative [8] or vibrational wave packet. After the excitation, the wave packet starts to move away from the equilibrium geometry. This makes production of the metastable trication via vertical short-pulse ionization inefficient. The longer the delay, the smaller the signal magnitude, in agreement with our observations.

As for the effect of the post-pulse, it is unlikely that weaker post-pulses further ionize the trications produced with the main pulse. To understand the experimental results we simulated the dissociation dynamics of the Cl_2^{3+} molecule solving the time-dependent Schrödinger equation on the two coupled charge-resonant surfaces $^2\Pi_g$ and $^2\Pi_u$. We used Cl₂ rather than I₂ since it is

much easier to calculate excited potential surfaces and especially accurate transition matrix elements for Cl_2^{3+}. We found that pulses with intensity of $\sim 10^{14}$ W/cm² lead to complete dissociation of Cl_2^{3+} bound states via the bond-softening mechanism [15] for pulses about 100 fs or longer. Thus, a relatively weak post-pulse will dissociate the molecular ion in agreement with the pump-probe experiment. The rapid decrease in efficiency of trication formation with long pulses is entirely consistent with the pump-probe experiment since the rising and falling parts of the pulse act like pre- and post-pulses, respectively, for the high intensity peak part of the pulse.

Although diatomic trications have been produced before [7,16], they have not been produced by optical means or in large quantities. Optical production is important since it opens the possibility for precision spectroscopy on this new class of simple molecules. The model that allows us to discuss the two-pulse experiments also allows us to address the spectroscopy of trications. Using strong-field femtosecond Raman spectroscopy, one can observe the modulation in the total amount of trications reaching the detector as a function of frequency difference between the two simultaneous femtosecond pulses. In general, the method consists of several steps which we will illustrate using the example of Cl_2^{3+}.

First, one has to establish a well-defined initial condition. If the ionizing pulse is short (e.g., 5 fs [17]) compared to the Cl₂ vibrational period, the ground state wave function of Cl₂ is transferred vertically to the bound surface of Cl_2^{3+} $[P(v = 0) = 77.4\%]$. However, in our case the main pulse is comparable to the vibrational period of the molecule. Consequently, it is hard to predict the vibrational distribution in Cl_2^{3+} after the pulse. To deal with this problem, a short pulse may be applied to "clean" all excited vibrational states without destroying the population of the $v = 0$ state. This is possible using the bond-softening mechanism [15]. In our numerical simulations based on solving the Schrödinger equation on the two coupled surfaces $^2\Pi_{u,g}$, a sin²-envelope FWHM = 150 fs pulse with peak intensity $I = 2.2 \times 10^{13}$ W/cm² and frequency $\omega = 1.17$ eV cleans 94% of the $v = 1$ state population (and 100% of $v > 1$ states population) leaving 92% of the $v = 0$ population intact.

For the spectroscopy step, two laser pulses with frequencies ω_1 and ω_2 and variable $\Delta\omega = \omega_1 - \omega_2$ are applied simultaneously. The pulse duration has to be long compared to the vibrational period of the trication. When $\Delta\omega \approx E(v = 1) - E(v = 0)$, the state $v = 0$ is significantly depleted and the population is transferred to excited vibrational states and the dissociative continuum (see Fig. 4). It is this $\Delta\omega$-dependent population transfer and dissociation that we propose to detect.

In the Floquet picture, vibrational excitation occurs due to the periodic oscillation of the dressed $^2\Pi_g$ surface at the beat frequency $\Delta\omega \approx \omega_{\text{vibr}}$. Depletion of $v = 0$ requires
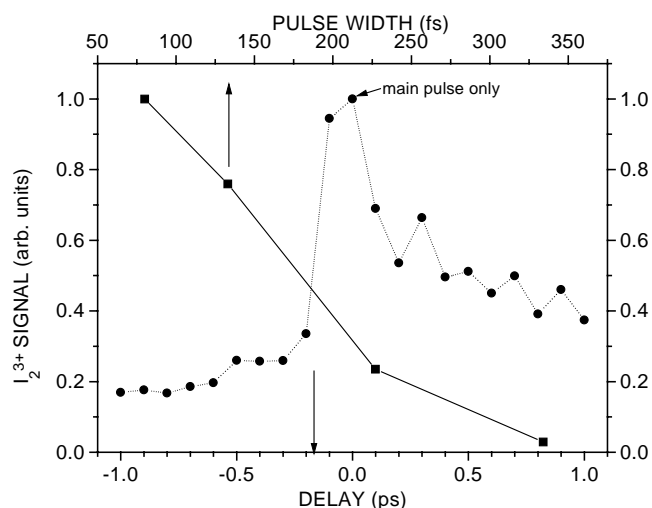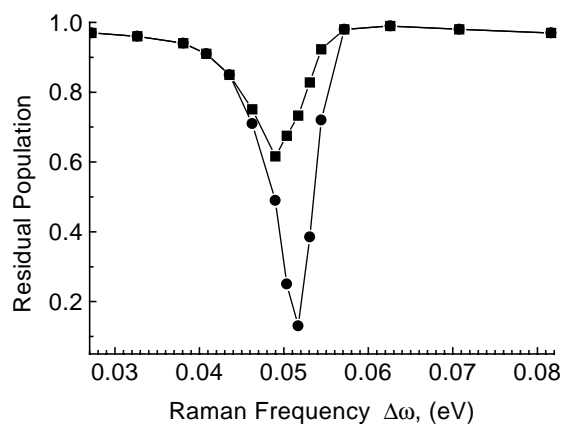

FIG. 3. I_2^{3+} signal vs pulse duration (squares, solid line, top axis) or vs the time delay between the two 80 fs pulses (circles, dotted line, bottom axis). Negative (positive) delay corresponds to a pre-pulse (post-pulse). Intensity is 3.6×10^{14} W/cm² for the main pulse and 1.2×10^{14} W/cm² for the pre- or post-pulses.

FIG. 4. Population of the $\nu = 0$ state (circles) and the total population of bound Cl_2^{3+} states (squares) after the pulse $\mathcal{E} f(t)[\cos(\omega_1 t) + \cos(\omega_2 t)]$ vs $\Delta\omega = \omega_1 - \omega_2$. The pulse parameters are $f(t) = \sin(\pi t/T)$, $T = 1.2$ psec (FWHM = 600 fs), $\mathcal{E} = 5 \times 10^7$ V/cm, $(\omega_1 + \omega_2)/2 = 1.17$ eV.

significant modification of the dressed $^2\Pi_g$ surface near R_e. However, nonresonant $^2\Pi_g - {}^2\Pi_u$ interaction near R_e becomes resonant at some $R_0 > R_e$ (see Fig. 2), causing strong overall suppression of a very weak bond. Hence, one has to maintain a balance between sufficient modification of the dressed $^2\Pi_g$ surface near R_e and keeping the $\nu = 0$ state bound on a dressed surface.

Figure 4 shows the results of our numerical simulations for $(\omega_1 + \omega_2)/2 = 1.17$ eV and a peak laser intensity of both ω_1 and ω_2 pulses (FWHM = 600 fs) equal to 3.5×10^{12} W/cm^2. The number of surviving trications (squares) is modulated by about 38%. The population of the ground state (circles) is modulated by about 85%. Applying a short "cleaning" post-pulse identical to the one applied at the first step will transfer the decrease in the $\nu = 0$ population into the decrease in the total Cl_2^{3+} signal, raising the modulation depth to about 85% and yielding better measurement of $E(\nu = 1) - E(\nu = 0)$. The redshift of the upper curve in Fig. 4 is due to the anharmonicity of the binding potential, both field free and induced by the Raman pulse. (The latter is hard to avoid unless the spectroscopy pulse is made very weak and long.)

In conclusion, ionizing molecules with little or no nuclear motion is at the heart of Coulomb explosion imaging [18]. Since efficient formation of diatomic trications is possible only with minimum nuclear motion, our results

imply that optical pulses can be a very effective ionization source for Coulomb explosion imaging. This means that the full power of pump-probe spectroscopy can be combined with Coulomb explosion imaging allowing time dependent structural changes of small molecules to be followed [8].

———

*Present address: Department of Chemistry, University of Aarhus, Langelandsgade 140, DK-8000, Aarhus C, Denmark.
†Present address: CPMOH/ELIA, Universite Bordeaux I, 351 Cours de la Liberation, 33405 Talence Cedex, France.
 [1] L. V. Keldysh, Sov. Phys. JETP **20**, 1307 (1964).
 [2] Y. Nagata *et al.,* Phys. Rev. Lett. **71**, 3774 (1993); B. E. Lemoff *et al.,* Phys. Rev. Lett. **74**, 1574 (1995).
 [3] D. Strickland *et al.,* Phys. Rev. Lett. **68**, 2755 (1992).
 [4] R. Weinkauf *et al.,* J. Chem. Phys. **98**, 8381 (1991).
 [5] P. J. Bruna and J. S. Wright, J. Phys. B **26**, 1819 (1993).
 [6] G. Handke, F. Tarantelli, and L. S. Cederbaum, Phys. Rev. Lett. **76**, 896 (1996).
 [7] K. L. Harbol, Ph.D. thesis, University of Kentucky, 1991.
 [8] H. Stapelfeldt, E. Constant, and P. B. Corkum, Phys. Rev. Lett. **74**, 3780 (1995).
 [9] C. Rolland and P. B. Corkum, J. Opt. Soc. Am. B **5**, 641 (1988).
[10] T. Seideman, M. Yu. Ivanov, and P. B. Corkum, Phys. Rev. Lett. **75**, 2819 (1995).
[11] D. M. Villeneuve, M. Yu. Ivanov, and P. B. Corkum, Phys. Rev. A **54**, 736 (1996).
[12] R. J. Buenker and S. D. Peyerimhoff, Theor. Chim. Acta **35**, 33 (1974); R. J. Buenker, Int. J. Quantum Chem. **29**, 435 (1986).
[13] R. J. Buenker and R. A. Phillips, J. Mol. Struct. **123**, 291 (1985).
[14] A. Bandrauk (private communication).
[15] P. H. Bucksbaum *et al.,* Phys. Rev. Lett. **64**, 1883 (1990).
[16] L. Morvay and I. Cornides, Int. J. Mass Spectrom. Ion Process. **62**, 263 (1984); D. L. Weathers *et al.,* Nucl. Instrum. Methods **B56/57**, 889 (1991); C. P. Safvan and D. Mathur, J. Phys. B **27**, 4073 (1994); K. Nagesha, V. R. Marathe, and D. Mathur, Chem. Phys. **154**, 125 (1991); T. T. Tsong and T. Kinkus, Phys. Scr. **T4**, 201 (1983).
[17] M. Nisoli *et al.,* Opt. Lett. **22**, 522 (1997).
[18] Z. Vager, R. Naaman, and E. P. Kanter, Science **244**, 426 (1989).